JMEPEG (2015) 24:4691–4695
DOI: 10.1007/s11665-015-1532-z

1059-9495/$19.00

A DNA-Assembled Fe_3O_4@Ag Nanorod in Silica Matrix for Cholesterol Biosensing

R.K. Satvekar, A.P. Tiwari, S.S. Rohiwal, B.M. Tiwale, and S.H. Pawar

(Submitted August 13, 2014; in revised form February 9, 2015; published online November 9, 2015)

A novel nanocomposite having DNA-assembled Fe_3O_4@Ag nanorods in silica matrix has been proposed for fabrication of bienzymatic cholesterol nanobiosensor. Cholesterol oxidase and horseradish peroxidase have been co-encapsulated in Silica/Fe_3O_4@Ag-DNA nanocomposite deposited on the indium tin oxide electrode. Cyclic voltammetry was employed for the electrochemical behavior of proposed biosensor and used to estimate cholesterol with a linear range of 5-195 mg/dL.

Keywords adhesion, casting, cholesterol nanobiosensor, enzyme immobilization, Fe_3O_4@Ag nanoparticles, silica nanocomposite

1. Introduction

Clinical disorders such as heart disease, hypertension, hypothyroidism, coronary artery disease, arteriosclerosis, and cerebral thrombosis, etc. occurring due to abnormal levels of cholesterol in the blood have stimulated public concern about the detection of cholesterol level. Therefore, there is an urgent need for a reliable biosensor to quantify the level of cholesterol in a blood sample rapidly (Ref 1). Improved electron transfer can be acquired by proper orientation of the enzyme on electrode surface and retaining native conformation. Many immobilization matrices are employed such as nanomaterials, sol-gel, and polymers have been reported for cholesterol biosensors. Among them, silica nanocomposite is a favorable candidate for the immobilization of enzyme, offering many advantages due to its unique chemical, physical, and electrochemical characteristics. The sol-gel technique provides a unique matrix in which various enzymes can be immobilized without loss of enzyme functionality (Ref 2).

Deoxyribonucleic acid (DNA) is a biopolymer, which has inherent self-assemble property, predictable base pairing, and high chemical stability that can transfer electron quickly between electrode surface and redox protein. Nanotechnology based on organic biopolymers including DNA is promising in various biomedical applications (Ref 3, 4). DNA-inorganic nanoparticle-based nanocomposite possesses biocompatible microenvironment around the enzyme. An electrochemically active species and metal ions specifically binds to double-stranded DNA provide unique electron transfer property improving electron transfer characteristics. Therefore, DNA is extensively employed as biorecognition elements in biosensors as well as unique building blocks in nanodevices (Ref 5). The stacked base pairs are considered as a system of π electrons; thus effective electron transfer inside the DNA duplex is possible over a distance up to 40 Å. Moreover, DNA has been used as easily flexible nanobiomaterial to construct defined hybrid nanocomposite (Ref 6). DNA strands, which serve as biocompatible scaffolds have high aspect ratios (length:diameter), charged nature, and recognition properties exploited for nanostructure formation (Ref 7). Interaction of DNA with magnetic nanoparticles is employed in various biomedical applications (Ref 8, 9). DNA-modified materials had been reported for immobilization of enzymes such as horseradish peroxidase (Ref 10) and glucose oxidase (Ref 11) for the fabrication of biosensors. Consequently, DNA is utilized as an economical, well-characterized, manageable, and easily adaptable material to construct defined hybrid nanocomposites.

In the present study, silver-coated magnetic nanoparticles (Fe_3O_4@Ag NPs) are synthesized in which Fe_3O_4 NPs (Magnetite) is a core and Ag NPs (Silver nanoparticles) is a shell. These are one of the most attractive core shell nanoparticles for its chemical activity and biocompatibility utilized in antibacterial activity (Ref 12) and immunoassay (Ref 13). Direct electrochemistry of cholesterol oxidase (ChOx) was achieved using a desirable nanocomposite based on DNA-assembled Fe_3O_4@Ag nanorods in silica matrix which is used to encapsulate HRP and ChOx.

2. Materials and Methods

2.1 Reagents and Apparatus

Double-stranded DNA was isolated from fresh ATCC 25922 *E. coli* culture. Cholesterol, cholesterol oxidase (ChOx, E.C. 1.1.3.6 25 U/mg), horseradish peroxidase (HRP, E.C 1.11.1.7, 100 U/mg), tetraethyl orthosilicate (TEOS), and indium tin oxide glass slide (~70-100 Ω, thickness 1.1 mm) were procured from Sigma Aldrich. Cholesterol, silver nitrate ($AgNO_3$), ferrous sulfate heptahydrate ($FeSO_4 \cdot 7H_2O$), and ferric chloride hexahydrate ($FeCl_3 \cdot 6H_2O$) were acquired from Hi Media, India. All other reagents were of analytical grade purchased from SD Fine Chemical Pvt. Ltd. India and used without further purification. The potassium phosphate buffer (0.2 M KH_2PO_4 + 0.2 M K_2HPO_4 + 0.1 M KCl) was utilized as supporting electrolyte for electrochemical analysis. All solutions were prepared with deionized double distilled water.

R.K. Satvekar, A.P. Tiwari, S.S. Rohiwal, B.M. Tiwale, and **S.H. Pawar**, Center for Interdisciplinary Research, D.Y. Patil University, Kolhapur 416006 MS, India. Contact e-mails: rajshrinaik5@gmail.com and pawar_s_h@yahoo.com.

2.2 Instruments

All electrochemical experiments were performed at a CHI 600 electrochemical workstation (CH Instruments Inc., USA) using a conventional three-electrode system with SiO_2/Fe_3O_4@Ag-DNA nanocomposite-modified ITO electrode, Ag/AgCl, and a platinum wire as the working, reference, and counter electrodes, respectively. Cyclic voltammograms were collected in a solution of potassium phosphate buffer containing 2-propanol 10% (v/v) and Triton X-100 0.7% (v/v). Transmission electron microscopy (TEM) images were captured with a Model: JEM-100 CX II opened at an accelerating voltage of 100 kV. UV-Vis experiments were performed with a UV-2100S spectrophotometer (Shimadzu, Japan).

2.3 Synthesis of Silver-Coated Iron Oxide Nanoparticles

The preparation of silver-coated Fe_3O_4 nanoparticles was carried out by two-step method: Initially, a core of 7 ± 2 nm Fe_3O_4 by the co-precipitation method was obtained. In a second step silver shell of 5 ± 1 nm using glucose as reducing agent was obtained. The Fe_3O_4 NPs were synthesized by chemical co-precipitation method as per reported elsewhere with some modification (Ref 14). Briefly, iron (III) chloride hexahydrate ($FeCl_3 \cdot 6H_2O$, 0.1 M) and iron (II) sulfate heptahydrate ($FeSO_4 \cdot 7H_2O$, 0.1 M) (1:1 Molar ratio) were mixed with strongly stirred NaOH (3.0 M) solution in deionized water at 88 °C for 15 min. The black precipitate product was magnetically decanted, and washed with ethanol and water. The prepared nanoparticles were dried at 60 °C for 6 h in a vacuum oven. Subsequently, Fe_3O_4 suspension (1.0 mg/mL was dispersed in 0.1 M Ag $(NH_3)_2^+$ solution and stirred for sufficient adsorption on Fe_3O_4 and 5.0 mg of glucose was added as reducing agent. Then the solution was heated in a water bath at 50 °C for 30 min. The slightly brown product was magnetically decanted, washed, and dried at 60 °C for 6 h in a vacuum oven.

2.4 Synthesis of SiO_2/Fe_3O_4@Ag-DNA Nanocomposite

The fresh DNA sample was isolated from fresh *E. Coli* culture using magnetic adsorption technology as per previous report (Ref 15). The isolated DNA was kept at 80 °C in a water bath for 10 min and then rapidly cooled in ice bath for 10 min for relaxing the supercoils. The double-stranded DNA was used for the preparation of Fe_3O_4@Ag-DNA nanorods. Freshly synthesized Fe_3O_4@Ag NPs were dispersed in DNA suspension in Tris-HCl buffer overnight. The resulting material was magnetically decanted, i.e., using a magnet the Fe_3O_4@Ag-DNA nanorods are separated and washed three times to ensure the removal of any unbound DNA. The sample was freeze dried for further characterization. DNA-assembled Fe_3O_4@Ag nanorods were then inserted into silica matrix, which was prepared to synthesize SiO_2/Fe_3O_4@Ag-DNA nanocomposite.

2.5 Fabrication of Cholesterol Bienzymatic Nanobiosensor

Prior to use, ITO plate was sonicated with acetone and ethanol solution, and washed with distilled water and dried at room temperature. Pre-cleaned ITO plates were immersed in a hydrolyzing solution of 1:1:5 (v/v) H_2O_2:NH_4OH:H_2O for about 30 min at 80 °C. After hydrolysis plates were rinsed with distilled water and dried at room temperature, the HRP solution (2.0 mg/mL) and ChOx (1.0 mg/mL) in potassium phosphate buffer of pH 7.0 were added to the SiO_2/Fe_3O_4@Ag-DNA nanocomposite solution for encapsulation of enzymes then coated onto a 1.0 cm^2 area of ITO electrode by drop casting method and kept at 4 °C for 12 h in the humid chamber.

The apparent enzyme activity (U/cm^2) was calculated using the method (Ref 16) based on the absorbance observed at 500 nm before and after the incubation of ChOx-modified electrode. The apparent enzyme activity 15.2×10^{-3} Abs/mg/dL was evaluated using Eq 1:

$$\alpha_{\text{app}}^{\text{enz}}\left(\text{U cm}^{-2}\right) = \frac{AV}{\varepsilon_{\text{st}}}, \qquad \text{(Eq 1)}$$

where A is the difference in absorbance before and after incubation, V is the total volume (3.08 cm^3), ε is the millimolar extinction coefficient (7.5 for o-dianisidine at 500 nm), t is the reaction time (min), and s is the surface area (1.0 cm^2) of the electrode. For measurement, a solution of 20 µL HRP, 10 µL of o-dianisidine solution, and 50 µL of 100 mg/dL cholesterol was diluted by adding 3 mL potassium phosphate buffer (pH 7.0) and was kept in a thermostat at 25 °C. The SiO_2/Fe_3O_4@Ag-DNA/HRP/ChOx/ITO electrode was immersed and was incubated for about 3 min.

3. Results and Discussion

The Ag@Fe_3O_4 NPs and SiO_2/Fe_3O_4@Ag-DNA nanocomposite were characterized by XRD, UV-Vis spectroscopy, TEM, and selected area electron diffraction (SAED). The XRD patterns of Fe_3O_4 NPs (a) and Fe_3O_4@Ag NPs (b) are illustrated in Fig. 1(A). As compared to the standard XRD pattern of Fe_3O_4 (ICDD Card no. 79-0419, magnetite) and Ag (ICDD Card no. 89-3722, face centered), the XRD pattern of Fe_3O_4@Ag NPs (c) displays diffraction peaks at 35.56°, 38.098°, 44.419°, 62.970°, 64.540°, and 77.362° which are assigned to (311), (111), (200), (440), (220), and (311). The results indicate that Ag@Fe_3O_4 nanoparticles composed of crystalline Fe_3O_4 and Ag. The crystallite sizes of nanomaterials were estimated from FWHM of the most intense peaks using the Scherrer formula. The crystallite sizes are found to be 7 and 12 nm for bare Fe_3O_4 NP and Fe_3O_4@Ag NPs, respectively. These results are consistent with the TEM results.

Figure 1(B) displayed the two strong characteristic peaks appeared at 420 and 260 nm in UV-Vis absorption spectra, which were assigned to Fe_3O_4@Ag NPs and DNA, respectively. Appearance of a peak at 260 nm in Fig. 1(B(c)) confirms that Fe_3O_4@Ag NPs had been successfully assembled on the DNA. The shape and position of the surface plasmon absorption band of silver nanomaterials are known to be intensely dependent on the particle size and dielectric medium. Conferring to Mie's theory (Ref 17), only a single SPR band is expected in the absorption spectra of spherical metal nanoparticles, whereas anisotropic particles could give rise to two or more SPR bands depending on the shape of the particles. Herein, a single SPR band is observed, which suggests that nanoparticles are spherical in shape and is consistent with the TEM observations.

The average particle size of Fe_3O_4 NPs (a) and Fe_3O_4@Ag NPs (b) is estimated to be 7 ± 2 and 15 ± 2 nm, respectively (Fig. 2a, b). TEM micrograph (Fig. 2c) illustrates that positively charged Fe_3O_4@Ag NPs is electrostatically attracted by the negatively charged phosphate backbone of DNA-forming nanorod structure of DNA-assembled Fe_3O_4@Ag NPs. The

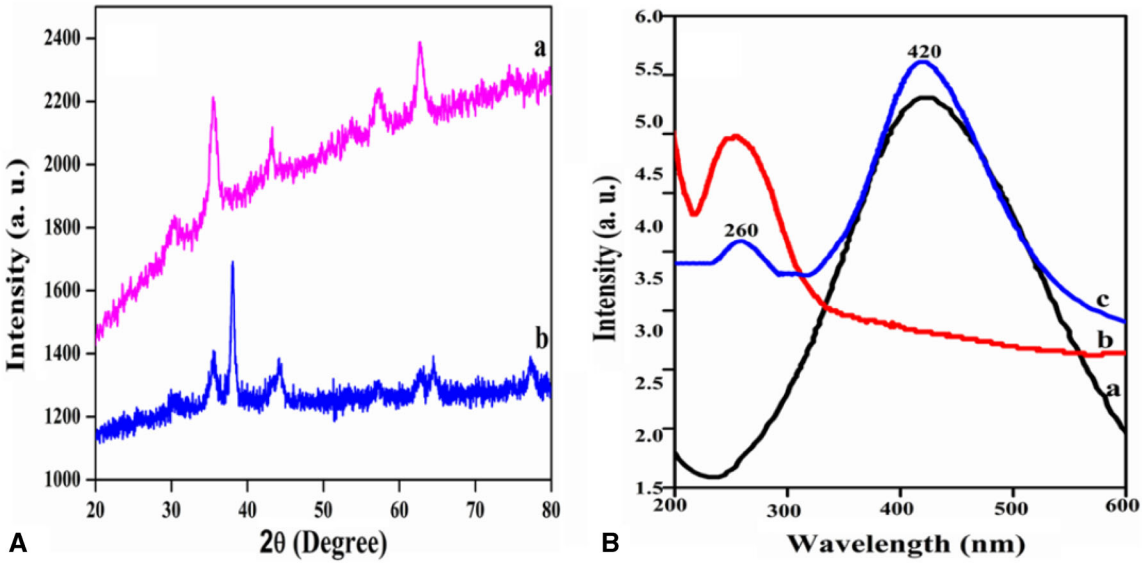

Fig. 1 (A) XRD pattern of (a) Fe_3O_4 NPs and (b) Fe_3O_4@Ag NPs; (B) UV Visible spectra of (a) Fe_3O_4@Ag NPs, (b) DNA solution in the buffer, and (c) Fe_3O_4@Ag-DNA nanorods

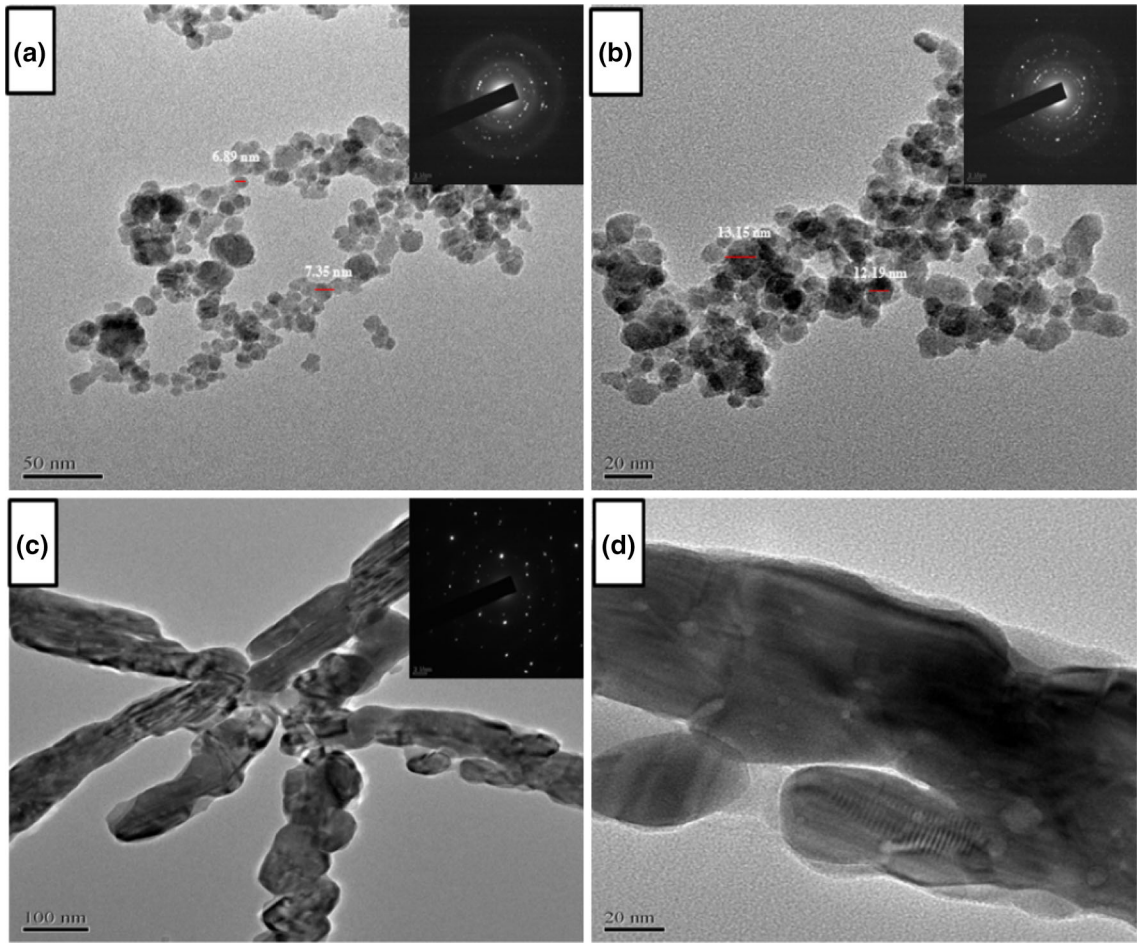

Fig. 2 TEM micrographs of (a) Fe_3O_4 NPs, (b) Fe_3O_4@Ag NPs, and (c) Fe_3O_4@Ag-DNA nanorods [inset SAED pattern of (a) Fe_3O_4 NPs, (b) Fe_3O_4@Ag NPs, and (c) Fe_3O_4@Ag-DNA nanorods]; TEM of (d) single Fe_3O_4@Ag-DNA nanorods

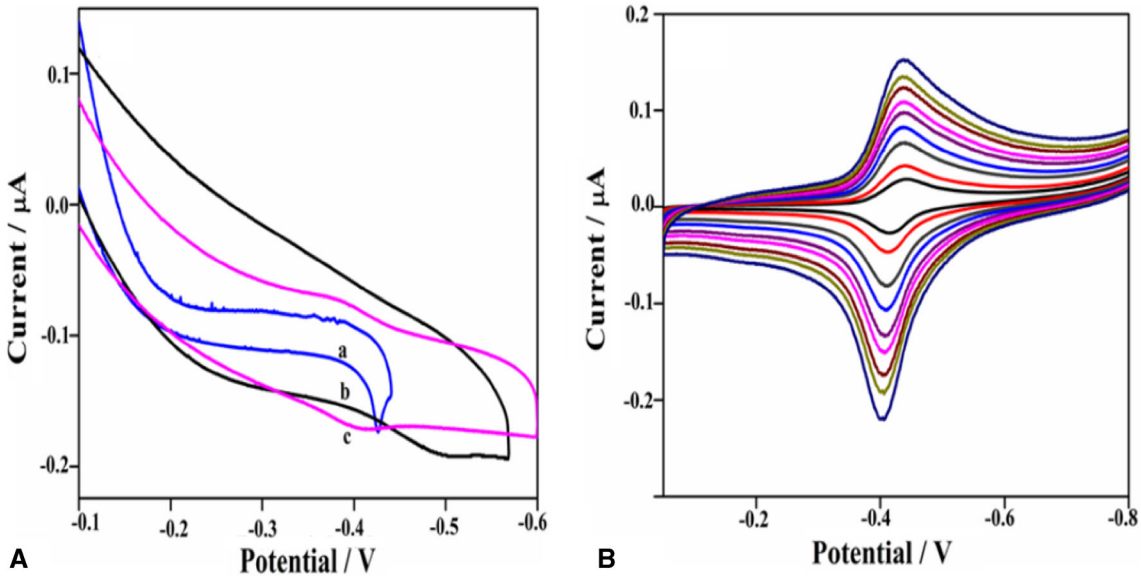

Fig. 3 (A) Cyclic voltammograms of modified electrodes (a) Fe_3O_4@Ag/ITO, (b) SiO_2/Fe_3O_4@Ag-DNA/ITO, and (c) SiO_2/Fe_3O_4@Ag-DNA/HRP/ChOx/ITO; (B) Cyclic voltammograms of the cholesterol biosensor in 0.1 M potassium phosphate buffer at varying scan rates

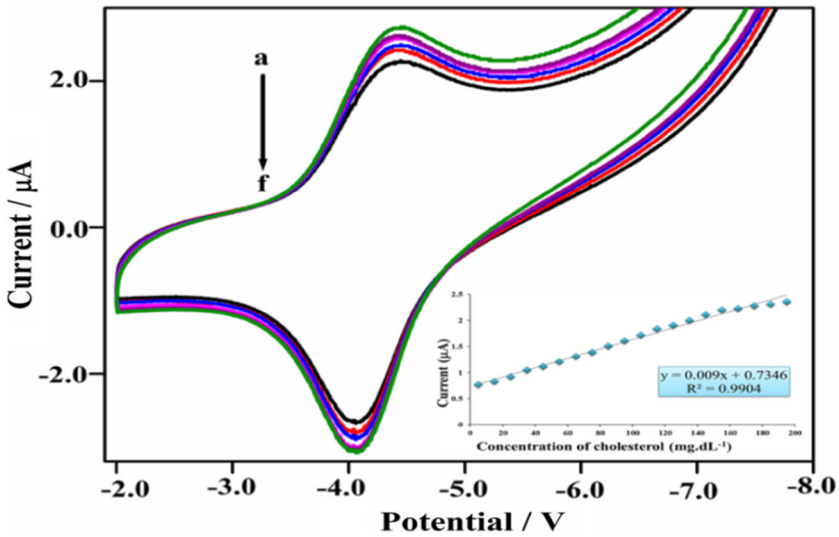

Fig. 4 Cyclic voltammograms of the SiO_2/Fe_3O_4@Ag-DNA/HRP/ChOx/ITO-modified electrode in potassium phosphate buffer of pH 7.0 containing different concentrations of cholesterol from a to f at 0.1 V/s [inset plot of catalytic peak current vs. cholesterol concentration in mg/mL]

SAED patterns of Fe_3O_4 NPs and Fe_3O_4@Ag NPs indicate the crystalline nature of materials while in Fe_3O_4@Ag-DNA nanorods; the intensity was decreased due to the amorphous nature of DNA. Figure 2(d) shows a TEM image recorded for single Fe_3O_4@Ag-DNA nanorods, demonstrating that the Fe_3O_4@Ag NPs grew along the DNA direction.

The cyclic voltammograms (CVs) of different modified electrodes in 0.1 M potassium phosphate buffer of pH 7.0 at the scan rate of 0.1 V/s is as displayed in Fig. 3(A). A small unsymmetrical reduction peak was observed at the Ag@Fe_3O_4-modified electrode (a), which indicated that Fe_3O_4@Ag was electroactive in the potential range from −0.2 to −0.8 V. While the SiO_2/ Fe_3O_4@Ag-DNA nanocomposite-modified electrode (b) having a very small single reduction peak suggested that the electrode was not reversible in this potential range. The SiO_2/ Fe_3O_4@Ag-DNA/HRP/ChOx-modified electrode (c) exhibited a pair of stable and well-defined redox peaks at −0.40 and −0.43 V (vs. Ag/AgCl), which could be attributed to the direct electron transfer of HRP encapsulated in the SiO_2/Fe_3O_4@Ag-DNA nanocomposite. The cyclic voltammetric responses validate that nanocomposite provides an auspicious microenvironment which preserves the biofunctionality of enzymes. Hence, the nanocomposite could improve direct electron transfer between enzymes and the underlying electrode surface. Furthermore, the redox peak current increases linearly with increase in scan rate for SiO_2/Fe_3O_4@Ag-DNA/HRP/ChOx-modified electrode indicating a typical surface-controlled electrode process as shown in Fig. 3(B).

The surface concentration of the SiO_2/Fe_3O_4@Ag-DNA/HRP/ChOx/ITO estimated from the plot of current versus potential using Brown-Anson model that is based on the following Eq 2 (Ref 18)

$$I_p = \frac{n^2F^2I^*AV}{4RT} \quad \text{(Eq 2)}$$

where n is the number of electrons transferred, F is the Faraday constant (96,584 C/mol), I^* is the surface concentration (mol cm^2) obtained from the SiO_2-DNA/Ag@Fe_3O_4/HRP/ITO electrode film, A is the surface area of the electrode (1.0 cm^2), V is the scan rate (100 mV/s), R is the gas constant (8.314 J^{-1} mol K), and T is the absolute temperature (298 K). The value of the surface concentration of the modified electrode has been found to be 10.709×10^{-6} mol cm^2.

The electro-catalytic properties toward cholesterol were explored on the SiO_2/Fe_3O_4@Ag-DNA/HRP/ChOx/ITO-modified ITO electrode. Fig 3(A) displays voltammograms in the absence and presence of cholesterol. When cholesterol was added, an obvious increase of peak current was observed, accompanied by the decrease of the oxidation peak current. The increment of reduction peak current became larger with the increasing cholesterol concentration. This indicated that the SiO_2/Fe_3O_4@Ag-DNA/HRP/ChOx/ITO electrode exhibited excellent catalytic activity for cholesterol. The catalytic reduction peak current increases with the linear calibration equation $y = 0.009x + 0.7346$ [mg/dL] ($R^2 = 0.9904$) in the range from 5.0 to 195 mg/dL of cholesterol (Fig. 4 inset). The sensitivity of modified electrode is 0.009 μA/(mg/dL) with detection limit 5.0 mg/dL.

The relative standard deviation of the SiO_2/Fe_3O_4@Ag-DNA/HRP/ChOx/ITO-modified electrode response to 15 mg/dL cholesterol was within 3.3% for six consecutive measurements, indicating that the biosensor had good reproducibility. The selectivity of proposed biosensor was evaluated by the interference study using 1:1 solution of cholesterol and interference substances. It was found that interfering substances glucose, ascorbic acid, and acetaminophen did not interfere significantly with the resulting biosensor, indicating that biosensor has sufficient selectivity.

4. Conclusion

A new biocompatible SiO_2/Fe_3O_4@Ag-DNA nanocomposite has been successfully synthesized for the immobilization of redox enzyme to study direct electron transfer. The method for the preparation of SiO_2/Fe_3O_4@Ag-DNA nanocomposite deals with some promising potential applications in nanocatalysis and nanoelectronics. The high sensitivity of the biosensor is attributed to the large surface area of Fe_3O_4@Ag for effective loading of enzymes as well as its high electron communication capability with the aid of enhanced selectivity and anti-interference ability due to the silica sol. The SiO_2/Fe_3O_4@Ag-DNA nanocomposite had remarkable compatibility with enzymes, but also good conductivity, so it exhibited excellent direct electrochemistry behavior.

References

1. S.K. Arya, M. Datta, and B.D. Malhotra, Recent Advances in Cholesterol Biosensor, *Biosens. Bioelectr*, 2008, **23**, p 1083–1100
2. R.K. Satvekar, S.S. Rohiwal, A.V. Raut, V.A. Karande, B.M. Tiwale, and S.H. Pawar, A Silica-Dextran Nanocomposite as a Novel Matrix for Immobilization of Horseradish Peroxidase, and Its Application to Sensing Hydrogen Peroxide, *Microchim. Acta*, 2014, **181**(1–2), p 71–77
3. S.S. Rohiwal, A.P. Tiwari, G. Verma, and S.H. Pawar, Preparation and evaluation of bovine serum albumin nanoparticles for ex vivo colloidal stability in biological media, *Colloids Surf. A Physicochem. Eng. Asp.* 2015, **480**, p 28–37
4. S.S. Rohiwal, R.K. Satvekar, A.P. Tiwari, A.V. Raut, S.G. Kumbhar, and S.H. Pawar, Investigating the influence of effective parameters on molecular characteristics of bovine serum albumin nanoparticles, *Appl. Surf. Sci.,* 2014, **334**, p 157–164
5. Hao Pei, Xiaolei Zuo, Dun Pan, Jiye Shi, Qing Huang, and Chunhai Fan, Scaffolded Biosensors with Designed DNA Nanostructures, *NPG Asia Mater.*, 2013, **5**, p e51. doi:10.1038/am.2013.22
6. Xu Shoujiang, Limiao Li, Du Zhifeng, Longhua Tang, Ying Wang, Taihong Wang, and Jinghong Li, A Netlike DNA-Templated Au Nanoconjugate as the Matrix of the Direct Electrochemistry of Horseradish Peroxidase, *Electrochem. Commun.*, 2009, **11**, p 327–330
7. H. Jaganathan, R.L. Gieseck, and A. Ivanisevic, Characterizing Proton Relaxation Times for Metallic and Magnetic Layer-by-Layer-Coated, DNA-Templated Nanoparticle Chains, *Nanotechnology*, 2010, **21**, p 245103
8. A.P. Tiwari, R.K. Satvekar, S.S. Rohiwal, V.A. Karande, A.V. Raut, P.G. Patil, P.B. Shete, S.J. Ghosh, and S.H. Pawar, Magneto-separation of genomic deoxyribose nucleic acid using pH responsive Fe_3O_4 @silica@chitosan nanoparticles in biological samples, *RSC Adv.*, 2014, **5**, p 8463–8470. doi:10.1039/C4RA15806G
9 A.P. Tiwari, S.J. Ghosh, and S.H. Pawar, Biomedical applications based on Magnetic nanoparticles: DNA interaction, *Anal. Methods*, 2015. doi: 10.1039/C5AY02334C
10. Y. Liu, L.M. Hu, and S.Q. Yang, Amplification of Bioelectrocatalytic Signalling Based on Silver Nanoparticles and DNA-Derived Horseradish Peroxidase Biosensors, *Microchim. Acta*, 2008, **160**, p 357–365
11. J. Leng, W.-M. Wang, L.-M. Lu, L. Bai, and X.-L. Qiu, DNA-Templated Synthesis of PtAu Bimetallic Nanoparticle/Graphene Nanocomposites and Their Application In Glucose Biosensor, *Nanoscale Res. Lett.*, 2014, **9**, p 99
12. Lingyan Wang, Jin Luo, Shiyao Shan, Elizabeth Crew, Jun Yin, and Chuan-Jian Zhong, Bacterial Inactivation Using Silver-Coated Magnetic Nanoparticles as Functional Antimicrobial Agents, *Anal. Chem.*, 2011, **83**(22), p 8688–8695
13. D. Tang, R. Yuan, and Y. Chai, Magnetic Core−Shell Fe_3O_4@Ag Nanoparticles Coated Carbon Paste Interface for Studies of Carcinoembryonic Antigen in Clinical Immunoassay, *J. Phys. Chem. B*, 2006, **110**(24), p 11640–11646
14. S.H. Gee, Y.K. Hong, D.W. Erickson, M.H. Park, and J.C. Sur, Synthesis and Aging Effect of Spherical Magnetite (Fe_3O_4) Nanoparticles for Biosensor Applications, *J. Appl. Phys.*, 2003, **93**, p 7560
15. A.P. Tiwari, S.J. Ghosh, and S.H. Pawar, Synthesis and Characterization of Functionalized Superparamagnetic Nanoparticles for Isolation of DNA, *Int. J. Pharm. Bio. Sci.*, 2014, **5**(3), p 533–542
16. R. Khan, A. Kaushik, P.R. Solanki, A.A. Ansari, M.K. Pandey, and B.D. Malhotra, Zinc Oxide Nanoparticles-Chitosan Composite Film for Cholesterol Biosensor, *Anal. chim. Acta*, 2008, **616**, p 207–213
17. J.P. Novak and D.L. Feldheim, Assembly of Phenylacetylene Bridged Silver and Gold Nanoparticle Arrays, *J. Am. Chem. Soc.*, 2000, **122**(3979), p 3980
18. A.J. Bard and L.R. Faulkner, *Electrochemical Methods: Fundamentals and Applications*, 2nd ed., Wiley, New York, 2000